

## BEHAVIOUR OF END SLABS IN CYLINDRICAL PRESTRESSED CONCRETE PRESSURE VESSELS

D. LANGAN, F.K. GARAS,

*Taylor Woodrow Construction Ltd., Southall, Middlesex, United Kingdom*

### ABSTRACT

The paper examines the general behaviour and shear failure mechanism of restrained thick slabs which form the end closures of cylindrical Prestressed Concrete Pressure Vessels. Typical results from a five year parametric study of over 20 model pilecaps are presented. In this work, the effects of bonded reinforcement, lined and unlined penetrations, span to depth ratio, concrete strength, level of hoop prestress and boundary conditions were investigated.

The factors which may influence the representivity of end slab tests and the effect of the significant parameters on the overload and ultimate load behaviour of the full scale structures are discussed.

Finally, the paper describes the components of internal shear resistance which balance the total shear force along the failure plane. Simplified design methods for determining the ultimate shear strength of end slabs are considered and related to the available test data.

### 1. INTRODUCTION

#### 1.1 General

After ten years of co-ordinated research, development and design, the use of cylindrical prestressed concrete pressure vessels for the containment of gas cooled reactors is now well established. A current tendency in reactor design is towards the adoption of higher internal pressures. Certain core refuelling layouts for high temperature reactors also demand a closer spacing of larger diameter holes which results in a greater loss of the cross sectional area of the slab than hitherto. In addition, with the introduction of the podded boiler layout, the walls of the cylindrical vessels increase considerably in stiffness and thereby create a higher degree of fixity for the pile cap.

Despite these more onerous conditions there is still no clear understanding of the overload behaviour and ultimate load mechanism of thick restrained slabs. A rational analysis has still to be developed which will reliably predict a lower bound failing pressure. A final assessment of the ultimate load factor must therefore rely exclusively on the performance obtained from model investigations.

Because of the lack of basic understanding of the failure mechanism there is a

tendency for the designer to be conservative and without exception end slabs for cylindrical pressure vessels have a considerable reserve of strength over the remainder of the pressure vessel.

End slabs are geometrically deep in relation to their diameter; span to depth ratios may be in the range of 2 to 3.5. The circular deep slabs are subject to flexure but the large deformations which would normally be induced are restricted by lateral restraint in the form of prestress and the rotational stiffness of the barrel cap connection. The shear forces on these elements under operating conditions may be several times higher than those occurring in conventional structures and because of the lateral restraint complex states of stress are produced. In the assessment of the ultimate strength of this type of element, the shear stresses are found to be dominant in determining the mode of collapse. The particular mode of failure is greatly influenced by the resistance of the concrete under complex states of stress.

The following table illustrates the main features of the end slabs of the various pressure vessels in service or now under construction.

TABLE 1.1 - MAIN FEATURES OF END SLABS IN P.C.P.V.

Vessel	Clear Span/ Depth Ratio	Barrel Thickness/ Cap Thickness	% Loss in Area Due to Penetrations	Design Pressure lb/sq.in.*
Oldbury "A"	3.50	0.68	4.4***	385
Dungeness "B"	3.24	0.62	6.1***	478
Hunterston "B"	3.44**	0.92	5.8	616
Hinkley Point "B"	3.44**	0.92	5.8	616
Hartlepool	2.39	1.17	17.5	644
Heysham	2.39	1.17	17.5	644
St. Laurence I	3.30**	0.66	unavailable	440
Bugey I	2.28	0.73	16.6	676
Chinon III	3.80	1.10	unavailable	440
Fort St. Vrain	2.02	0.58	24.6	845

\*  $N/mm^2 = 145 \text{ lb/sq.in.}$

\*\* Neglecting increased thickness at edge of cap/haunch

\*\*\* Estimated values - control rod tubes were not included

In the majority of the vessels described above the barrel cap thickness ratio varies between 0.58 to 0.92 whereas for the Hartlepool and Heysham pressure vessels this ratio is 1.17 as the boiler pods are contained in the barrel walls.

The basic depth of the cap can be chosen with reference to completed research information on the behaviour of model pile caps or on the experience of previous full scale designs. In selecting the dimensions and the specific arrangement of prestressing tendons emphasis is generally placed on establishing a favourable distribution of stress under normal operating conditions. Two alternative approaches are possible :

- a. Prescribe an allowable concrete stress level which cannot be exceeded whether bonded reinforcement is used or not. This approach effectively prevents or severely limits any external cracking on the surface of the vessel.
- b. Design on the basis of a partly prestressed concrete slab in which the reinforcement stresses are those normally accepted in reinforced concrete practice (or possibly restricted to those for water retaining structures). The amount of reinforcement can then be calculated which must be consistent with the feasibility of placing the bars within the ligaments between the standtube penetrations and obtaining a fully compacted concrete.

For both alternatives an additional small percentage of reinforcement can be introduced to take account of shrinkage effects, thermal stresses etc. In general, the first approach is normally adopted so that the operating stresses control the thickness of the pile cap and the overall safety has subsequently to be determined by experimental analysis.

## 2. POSSIBLE MODES OF FAILURE

From the authors experimental work and the examination of that of other researchers (references 1 - 6) the following modes of failure develop when deep restrained circular slabs are pressurised to failure, (Fig.1).

Flexural cracking first occurs but the radial yield lines which are produced develop an extremely high moment of resistance as the compression zone across each yield line is in a state of triaxial stress. The ultimate bending moment is therefore not attained and a yield line collapse does not generally occur in thick slabs with span to depth ratios below 3. The mode which initially develops is invariably preceded by one of two other collapse mechanisms viz:

- (i) The rotation of the ring beam or edge of the slab increases such that the hoop prestress fails in simple tension across one of the vertical cracks in the edge of the barrel.
- (ii) If the ultimate strain capacity of the prestress is not exceeded then a central core of concrete is displaced and isolated from the main annulus of concrete. The position of the plane is governed by the location of the vertical prestress; the inclination by the hoop prestress and span to depth ratio.

Two basic forms of shear failure may be identified: shear compression failure which takes place when the compression zone is gradually reduced in size due to inclined cracks. The remaining section which is under a compressive field stress fails by sliding along planes effectively in line with the applied load. Alternatively the principle tensile stress creates an inclined crack across the compression zone at the point of collapse.

## 3. REVIEW OF PREVIOUS WORK ON END SLABS

Studies on the behaviour of end slabs have been carried out and reported over the last four years by at least 5 groups of research workers.

Brading and Hills (reference 1) presented results of 6 models, two of which were reinforced slabs. The other four 1/24th scale models had a span to depth ratio of 2.9, and were of specific designs of prestressed circular slabs. The purpose of the tests was

to provide information for the design of the "Dungeness B" vessels. Only one model was pressurised to failure; tests on the remainder were discontinued mainly because of leakage in the liner of the pressurising system.

Morgan (reference 3) indicated that about 12 models slightly more than 2 ft. (610 mm) in diameter were tested for checking the design of the Oldbury and Hinkley Point "B" pressure vessels. No experimental details or results were given, however it was stated that shear failure did not take place in any of the models.

Campbell-Allen (references 2 & 4) carried out two types of experiments. In type I seven slabs were tested with an overall diameter of 34 in. (863 mm) and clear span to depth ratios of 3.67 and 1.835. The hoop prestress, which ranged between 1210 and 3500 lb/sq.in. (8.35 and 24.10 N/mm<sup>2</sup>) consisted of straight tendons either 0.200 in. or 0.276 in. (5.1 or 7 mm) diameter in unlined ducts. In the second type a number of small discs and skirted slabs were loaded to failure. The prestress was applied by external bolts acting against either one or a series of octagonal stiff rings. By plotting the results obtained from the two types of experiment (reference 7) it can be seen that for similar span to depth ratios and amounts of restraint, the failing pressures of the small scale specimens were almost double those obtained from realistic slabs (Type I). It is believed that the increased stiffness induced in the small specimens by restraining ring and bolts accounted for the major difference in results.

To date 25 tests have been carried out by the University of Illinois (reference 5) on skirted prestressed concrete slabs. The investigations covered a range of span to depth ratios (1.67 to 5) and the amount of hoop restraint varied between 220 and 1290 lb/sq.in. (1.52 - 8.90 N/mm<sup>2</sup>). Eight of these slabs failed in shear and the remaining slabs either failed in flexure or the tests were discontinued because of leakage in the pressure system. The reason for the high percentage of liner leakages is believed to be due to the use of long length of barrel and lack of sufficient hoop forces to prevent the large displacement of the barrel stub.

Finally, Meerwald and Schwiers (reference 6) reported a test on a 1/20th scale model of a perforated prestressed concrete end slab with a span to depth ratio of 3.1. The applied hoop prestress was about 1500 lb/sq.in. (10.30 N/mm<sup>2</sup>). Failure took place when the central core was forced out at a pressure of 2850 lb/sq.in. (196 N/mm<sup>2</sup>).

#### 4. EXPERIMENTAL WORK

As part of a general development study into the structural behaviour of pressure vessels for the containment of advanced and high temperature gas cooled reactors, a comprehensive programme of experimental work to examine the shear mechanism of restrained thick circular slabs has been completed; this is summarised in Table 4.1. The five year study has included the examination of the major parameters affecting the ultimate strength and mode of failure of end slabs viz:

- a. Bonded reinforcement
- b. Presence of lined or unlined penetrations in the pressurised zone.
- c. Presence of the penetrations in the barrel wall.
- d. Concrete strength.

- e. Level of hoop prestress
- f. Pressurised penetrations in the standpipe zone.
- g. Boundary conditions.
- h. Sustained elevated temperature.

#### 4.1 Experimental Details

For all the models tested the hoop prestress was applied by continuous windings of wire with the exception of two models of the bottom cap of the Fort St. Vrain reactor pressure vessel (models G1 & G2) where internal crosshead tendons were used. Crushed limestone concrete with  $\frac{3}{8}$  in. (9 mm) maximum size was used in the majority of the models. Each model was vertically prestressed onto a thick concrete base. For most models the vertical prestress was represented by replacing sets of full scale tendons by single high tensile bars. All other experimental details and dimensions are given in Fig.2.

Uniform pressure was applied to the inner surface of each model by means of a completely enclosed rubber pressure chamber. All models were subjected to a number of pressure cycles before proceeding to failure.

The deflected profile of each model was measured during pressurisation along two diameters at the outer surface of the cap, and along the adjacent sides of the barrel stub. Electrical resistance gauges were used to measure strains at the inner and outer surfaces of each cap and within the concrete mass to observe the development of internal cracking. These measurements provided information on the changes in the depth of the compression zone with increasing pressure. Vibrating wire gauges were mounted across the haunch to indicate the development of the circumferential cracks along the two edges of the haunch. Strains were also measured at critical regions on the reinforcement, standpipes and boiler penetration liners, where they were included.

#### 4.2 Flexural Behaviour

The general behaviour of an end slab is shown in Fig.3 where the central deflection, as a percentage of the value at ultimate is plotted against percentage of maximum pressure. Deflection profiles for models C2 and C4 are shown in Fig.4. The flexural behaviour of the slab may be divided into three stages. The first stage, elastic, is defined by the pressure at which the first radial cracks formed on the external surface. This pressure varied between 40 and 62% of the ultimate pressure when the central deflection was equivalent to about 5% of the maximum, ( $\frac{1}{450}$  of the depth).

During the first stage haunch cracking occurred. From the vibrating wire gauge measurements it appears that these cracks formed at pressures between 37 and 59% of the ultimate pressure. The strain measurements confirmed that these cracks first occurred at the edge of the haunch adjoining the barrel. The formation of these cracks however, did not influence the linearity of the deflection profile of the slab.

The second stage, elastoplastic, was characterised by the development of external flexural cracks. The cracks started at the centre of the slab and spread towards the edges of the cap; on average they were fully developed at about 74% of the ultimate strength. Further pressures caused secondary cracks to appear between the major radial cracks. Fig.5 gives a typical development of flexural cracking.

Further pressure 70 to 80% of the ultimate caused a rapid increase of deflection due to yielding of the tensile reinforcement in the central region. This yielding progressed from the centre to the edges of the cap in the pressure range 70 to 90% of the ultimate.

In all the pile caps, the barrel stub cracked longitudinally. These cracks were first observed at pressures between 59 to 74% of the ultimate. The pressure at which cracking occurred and its extent were dependent on the rotation of the ring beam. Generally, the cracks started at the extreme top of the slab and extended downwards towards the bearing face of the barrel stub. The strains measured from the embedded gauges and those on the tensile reinforcement indicated that inclined cracks formed internally at pressures of about 55% of the ultimate. The inclined cracks probably extended rapidly up to 80% of the ultimate pressure and then developed more slowly.

In the final stage, yielding of the reinforcement was fully developed along all the radial cracks and the deflections increased considerably with a small increase in pressure; the maximum deflection varied between 0.4 and 0.5 in. (10 and 12.5 mm). In some of the tests hoop cracks next to the anchorage plates and between the anchorages were observed at pressures ranged from 74 to 95% of the ultimate.

Although flexural plastic stage was well advanced it did not result in failure as another mode interceded i.e. a central plug of concrete was extruded through the circular slab (see Fig.6 to 9).

#### 4.3 Mode and Mechanism of Failure

Failure was considered to occur when the circular area of concrete adjacent to a line which inscribed the vertical prestress anchorage plates, was displaced vertically with the formation of a distinct step around its edge, see Figs. 6 to 9. At this stage flexural cracking was complete and the internal pressure could not be sustained.

From the differential deflections observed on both sides of the shear plug failure plane there was an indication that the central core began to develop at about 78% of the ultimate pressure, (see Fig.10). Examination of the inner surface of the models showed, (Figs. 11 & 12):

- a. Two circumferential cracks along the edges of the haunch fillet; the development of the strain across the two cracks is shown in Fig.13.
- b. An annular zone of striated concrete. The diameter of this circular zone was 9 to 10 in. with a radial thickness of approximately 2 in. (50 mm) for both perforated and unperforated pile caps. Fig.12 shows that a distinct step occurred in this area which accounted for most of the total external displacement of the plug i.e. the main shear failure plane terminated in this zone of concrete.
- c. In certain unperforated models the inner 1 to 2 in. (25 to 50 mm) of concrete adjacent to the pressurised face and within the shear plug diameter was severely dislocated and crushed. This crushing was not immediately apparent and could only be observed after removal of the central core.

After failure some of the models were sliced to study the crack patterns initiated inside the concrete mass and to further evaluate the mode of failure, Fig.14. Examination

of the sections showed that :

- (i) A truncated conical plug like failure occurred which produced a marked step on the outer surface of the slab associated with visible cracking on the inner surface.
- (ii) The angle of the shear plane varied between  $26^{\circ}$  and  $30^{\circ}$  to the vertical.
- (iii) Haunch cracks formed at angles of  $25^{\circ}$  and  $36^{\circ}$  to the horizontal. The major crack propagated from the junction of the haunch splay and the barrel and extended most of the way through the thickness of the ring beam. The second crack propagated less than 2 in. (50 mm) into the cap.

## 5. PROBLEMS OF REPRESENTIVITY AND EFFECT OF MAJOR PARAMETERS

Although experiments on model end slabs cannot represent exactly the conditions that arise in the complete vessel, they give an approach for examining the ultimate strength and mode of failure. The following is therefore a brief discussion of the key factors which may influence the representivity of end slab tests and the effect of those parameters on the overload and ultimate load behaviour of the full scale structure.

### 5.1 Boundary Conditions

5.1.1 Effect on flexure: The major difficulty with testing an isolated end slab of a pressure vessel is to determine what boundary conditions should prevail as it approaches structural failure, and secondly, what boundary conditions do actually occur in the experimental testing of such a slab.

The significance of boundary conditions on the initiation of the flexural cracks and the deflected form of the end slabs has been demonstrated in the authors' work on complete vessels and isolated slabs with and without barrel stubs, (see Fig. 15 and 16). The boundary conditions were varied by changing the pressurised length of the barrel stub, the pre-load in the vertical prestress and the amount of lateral restraint. The quantity of bonded reinforcement at the haunch also affects the pressure at which flexural crack initiate but this effect has not been examined.

These various factors influence the rotation of the ring beam of the cap which results in a differential increase in the load in the hoop prestressing tendons. The rotation of the ring beam produces vertical cracking at the extremity of the barrel. The extension of the tendons due to the radial displacement is, therefore, locally increased at the cracks. Beyond a given rotation, progressive prestress failure will therefore occur, followed by a yield line collapse or a shear type failure of the concrete.

In this investigation the end slabs had a short length of barrel stub which accelerated the development of the radial cracks at the outer face of the slab. Cracking was observed in the isolated caps at pressures between 1200 and 1500 lb/sq.in. ( $8.2$  and  $10.3$  N/mm<sup>2</sup>) whereas in a complete 1/10th scale model of the same design (reference 8) a pressure of 1800 lb/sq.in. ( $12.4$  N/mm<sup>2</sup>) only produced a single short crack adjacent to the central ligament. The effect of pressurising different lengths of barrel stub was examined in the case of models G1 and G2. When a short length of barrel was pressurised flexural cracking first occurred at 2200 lb/sq.in. ( $15.2$  N/mm<sup>2</sup>) whereas when the complete barrel

was pressurised no radial cracks were observed until a pressure of 2600 lb/sq.in. ( $17.9 \text{ N/mm}^2$ ). The difference in the behaviour can be accounted for by the change in the edge fixity which controlled the rate at which flexural cracks developed.

5.1.2 Shear behaviour: The most likely failure of end slabs with span to depth ratios of less than 3 is a shear mode. When examining the effect of boundary conditions on the shear stresses which develop across the potential failure plane (see Fig.17), the combined action of the compressive zone and the aggregate interlock of the tensile zone, in resisting shear stresses, should be considered.

From the authors' work on models and from the assessment of published data (references 8 to 10) on the behaviour of cylindrical prestressed concrete pressure vessels it has been shown that the rotation of the ring beam in a complete vessel is small so that prestress failure is unlikely, and, therefore, any boundary conditions which could lead to flexural failure of the head may not be representative.

Two extreme cases of end slab behaviour may be considered i.e. when the maximum rotation of the ring beam is small (say 1% extension of the prestress) and the second when this rotation causes (say 3 to 4% extension). If the depth of the compression zone is different for the two amounts of rotation, it is possible that the summation of the shear compression and aggregate interlock effect are similar. Further experimental work on the aggregate interlock in deep sections is required to substantiate this argument.

In assessing the ultimate shear strength of end slabs from published data on the behaviour of realistic models it appears that the influence of lateral prestress is very small. A study of restrained deep beams with a span to depth ratio of 2.5 has similarly indicated that both the edge rotation and the prestress level at ultimate had little effect on the shearing strength (reference 11). In this work, an increase in the restraint from zero to 6% of the cylinder strength ( $f'_c$ ) improved the shear strength by more than 30 times. This was due to a change from flexural failure to jammed shear compression failure caused by the compressive membrane action. Once this mode is dominant a further increase of restraint has only a small effect e.g. 24%  $f'_c$  only produced an additional 19% in the shear strength.

A further uncertainty in end slab behaviour is whether the depth of the compression zone prior to failure varies with change in rotation of the ring beam or lateral restraint. From the beam tests there was an indication that the depth of the compression zone at ultimate was similar for lateral restraint, ranging from 600 to 2500 lb/sq.in. ( $4.1$  to  $17.2 \text{ N/mm}^2$ ).

This evidence appears to show that the effect of varying the boundary conditions on the ultimate shearing strength of the cap may not be significant.

## 5.2 Span to Depth Ratio

An increase in the thickness of the slab in relation to its span has a dominant effect on increasing the ultimate shearing strength since it is a function of the area of concrete available to resist shear. Reducing the span to depth ratio in models C4 and M0 from 2.5 to 2.0 increased the shear strength by 20%. Similar conclusions on the influence of this factor on the shear behaviour of end slabs can be drawn from references

2 and 5. For example, by halving the span to depth ratio but maintaining the same level of hoop prestress the ultimate strength was increased by 130%.

### 5.3 Vertical Prestress

In the investigation described the vertical prestress was simulated by a small number of high tensile bars as mentioned in 4.1. Each bar was positioned at the centre of action of the group it replaced and the bearing plate covered a geometrically similar area to the total anchorage zone it simulated. The arrangement was considered to be reasonably representative of the multiple anchorages in the prototype. This conclusion has been confirmed by the testing of model C10 where each vertical tendon in the prototype was simulated by a single 0.2 in. diameter prestressing wire. The mode of failure and the ultimate strength of this model was very close to similar models (C4, C7) which were prestressed with a small number of high tensile bars.

As described in section 4 the exit of the shear plug was controlled by the position of the anchor plates. The ultimate shearing strength may be increased by reducing the shear span or distance between the anchorages. Similar conclusions have been derived from previous experimental work on the punching shear failure of flat slab structures (reference 12). It is therefore desirable in pressure vessels that the vertical prestress tendons be curved around the haunch. This has the advantages of reducing the shear span, increasing the compressive forces in the cap and delaying the formation of the haunch cracks.

### 5.4 Hoop Prestress

If failure of the lateral prestress is a possible mode of collapse it is essential that the stress strain characteristics (yield stress, proof stress and maximum strain) of the prototype and model tendons be the same. To model the crack width the frictional properties between the prestressing tendons and the ducts or winding channels should be simulated as closely as possible.

Lateral restraint or hoop prestress increases the ultimate strength of concrete subject to shear. The rate of increase in shear strength is not, however, directly proportional to the rate of the increase in the restraint. Beyond a certain level any increase in the restraint has negligible effect on the shear strength. This has been confirmed by experimental work on the behaviour of restraint deep sections (reference 13). Furthermore, analysis of published tests on end slabs (reference 2) has shown that by increasing the prestress level above 1200 lb/sq.in. the ultimate pressure only increased by 4%.

### 5.5 Penetrations

Because of the impracticability of scaling the ligament between the standtubes of the full scale structure the majority of model pile caps (C1 to C10) described in Table 4.1 had 21 simplified standtubes to simulate the same effective modulus as the prototype i.e. the pitch to diameter, liner thickness to diameter ratios were held constant. The loss in area due to the holes was also scaled.

Whilst this arrangement simulates the elastic stiffness it has not yet been verified that it reproduces the full scale behaviour in the plastic conditions. This effect is currently being investigated by comparing the behaviour of two models of the same design. The ratios described were maintained constant for models M0 and M1 but 55 and 155 tubes

were included. The central deflections of these two models up to a pressure of 1800 lb/sq.in. is shown in Fig.18.

In all the perforated end slab models the failure plane intersected the outer row of standtubes. However, the ultimate pressure was only 10% lower than that for the unperforated models. This small reduction was probably because the dowel action of the standtubes partly compensated for the loss of cross sectional area of concrete acting in shear. In model C9 the penetrations were unlined which resulted in a 28% reduction of the ultimate strength. As seen in (Figs. 7 and 9) at failure the central truncated plug of concrete slid over the outer row of liners which were locked into the remainder of the cap. The provision of shear connectors could therefore increase the ultimate strength of perforated pile caps. The small effect of perforations on the ultimate pressure is also supported by tests completed at the University of Illinois, (reference 5).

### 5.6 Temperature

There is no experimental evidence available on the effect of temperature on the ultimate shear strength of end slabs. Sustained temperature, however, may influence the strength in two ways :

- a. By causing degradation of the concrete which may result in reduction in strength.
- b. By causing excessive loss in the lateral prestress. This has been examined in models C11 and C12 where the stress at transfer was reduced from 600 to 360 lb/sq.in. ( $4.1$  to  $2.5$  N/mm<sup>2</sup>) whilst maintaining the same area of steel. The difference between the ultimate shear strength was only 10%.

The effect of sustained temperature on the ultimate shearing strength of end slabs is being investigated in models M1 and M2 and it is hoped that the results will be available during the general discussion of this paper.

### 5.7 Concrete Strength

Since the primarily purpose of end slab tests is to examine the overload and ultimate load behaviour, the model concrete should have similar elasto-plastic behaviour under complex stress to that of the full scale concrete. The crack propagation should be similar as well as the range of plasticity as a percentage of the total strength.

The maximum aggregate size may have an influence on the shear strength of concrete structures because of interlock action. When a crack forms in an end slab the shear displacement probably causes the larger aggregate particles to act as dowels. The dowel forces produced by the interlock are a function of the contact area in bearing between the aggregate particles across the crack and the surrounding cement matrix. Work on the effect of aggregate size on the failure of concrete under triaxial compression has shown that the shear strength increases with the maximum size of aggregate (reference 14).

Fenwick (reference 15) has shown that for any given shear displacement the shear resistance increases with improvement of concrete strength and as the crack size diminishes.

The relationship between the shearing strength of structural members e.g. beams and slabs and the compressive strength of the concrete has been examined by many investigators. In most of the design equations which were developed for beams and slabs the shear strength

has been related to the square root of the compressive strength. As the tensile strength of concrete is approximately proportional to  $\sqrt{f_c}$ , (reference 16) the dependency of shearing strength on the same factor is reasonable. Similar views were presented by Moe, Hognestad and Morsch for (references 12, 17 and 18) structural members failing in shear.

The effect of concrete strength on the maximum shear strength was examined in models C1, C2, C11 and C14 where  $f_c$  varied between 3000 and 8000 lb/sq.in. (21 and 55 N/mm<sup>2</sup>). The ultimate pressure was found to be proportional to the square root of the compressive strength. A similar conclusion has been drawn from the study of small deep restrained elements (reference 13).

#### 5.8 Bonded Reinforcement

Ideally, it is desirable to scale down each individual bar so as to maintain the stress and bond scale factors. The practicability of model construction does not generally permit this and one model bar has to represent a number of full scale bars. This approach is adopted in most models of complex structures since it is believed that cracking does occur at the same scaled load as in the prototype.

Generally, flexural cracking occurred in the slabs at pressures higher than twice the design pressure. When considering the development of cracks due to pressure in excess of this value it is likely that the presence of multiple penetrations and other geometry changes produce their own crack pattern because of stress concentration effects. The presence of reinforcement is, therefore, unlikely to modify greatly the extent of cracking in the overload stages.

It has been demonstrated by models C4 and C5 that the contribution of the reinforcement towards the ultimate load of thick slabs is very little. Surface reinforcement equivalent to 0.44% of the cross sectional area of the slab only increased the ultimate shearing strength by 3% presumably because of the dowel forces. These forces, by calculation, have been shown to be negligible compared with the total forces acting on the slabs.

### 6. ASSESSMENT OF SHEAR RESISTANCE

Because of the low span to depth ratio flexural failure is unlikely in the end slabs of cylindrical prestressed concrete pressure vessels. Shear failure is a characteristic of thick slabs and occurs before the flexural capacity is exhausted. In the following discussion the components of internal shear resistance which balance the total shear force along the failure plane are identified. A discussion of the likely range of values of each component is presented. In addition, three simplified design methods for determining the ultimate strength of end slabs in shear are considered and related to the results of the experimental work carried out by the authors and other researchers. The limitations of each method are also discussed.

To assess the lower bound failing pressure two approaches are possible for the development of general design rules. The first is to derive a mathematical approximation to the particular mode of failure observed from the testing of models under determinate boundary conditions. If this is not feasible the alternative is to undertake a parametric experimental study and relate all results non-dimensionally. This may lead to an empirical

formula based on a statistical analysis of the data.

Because the amount of data available on the ultimate load behaviour of restrained deep slabs is still too limited to enable comprehensive design rules for shear to be developed, the second alternative is more realistic at this time.

### 6.1 Information Required for Analysis

To produce a simplified analytical expression for determining the ultimate load of end slabs the following quantities are required:

6.1.1 The position of the shear plane at failure: In the majority of experiments the shear plane emerges at the inside edge of the vertical prestress anchorage zone. It takes the form of a truncated conical plane through the section which in some cases is interrupted by an additional vertical cylindrical plane. The angle of the plane is influenced by the applied stress and the span to depth ratio.

6.1.2 The state of stress along the shear plane: It is possible to measure the distribution of internal strain at a number of points within a model e.g. in the experimental work described in section 4 approximately 100 internal strain measurements were recorded in the majority of the model pile caps from which the zones of tensile strain have been interpolated (see Fig.19).

It has been found that the development of tensile strain does not necessarily infer that cracking had occurred or that the concrete could not resist shear. During the authors work on concrete subjected to multiaxial states of stress, tensile strains in the range 1000 to 3000 microstrain were measured without visible cracking. The main problem therefore, is to determine the limiting tensile strain in a complex stress field beyond which cracking would occur. In thick slabs with very high shear moment ratios, the amount of flexural cracking at the onset of shear failure will be smaller than for conventional slabs.

For a more precise estimate of the shear capacity of the compression zone of the pile cap the distribution of stress transmitted from the hoop prestress to this area is required. The controlling factor is the position and extent of the haunch crack.

6.1.3 The Shear resistance of the concrete in relation to the field stress: The simplest approach is to adopt the classical relationship for concrete failing in principal tension. No data however exists for the maximum value of principal tensile stress for concrete under a system of complex restraint. Fig.20 relates shear resistance to field stress. The first curve is a mean value for the ultimate strength of concrete discs where the failure plane was conditioned to be normal to the applied load (reference 13). The lower curves are for the failure of the same concrete in principal tension. Conditions in the pile cap probably lie between these two extremes.

### 6.2 Mechanism of Shear Resistance

The total shearing force  $F$  is resisted by the component forces shown in Fig.17.

6.2.1 Shear resistance of the compression zone ( $F_c$ ): From the extensive amount of surface and internal strain measurements within all the pile caps, it was possible to determine the reduction in depth of the compression zones with increase in internal pressure. Fig.19 illustrates the tensile and compressive zones with varying pressures.

At the point of failure it is anticipated that the depth of the compression zone was reduced to about 15% of the original depth of the slab, and Fig.21 represents average values for the depth of the compression zone in the pressurised area with increase in pressure.

6.2.2 Shear transfer by the vertical components of the aggregate interlock within the tension zone ( $F_g$ ): This action develops because of a shear displacement parallel to the direction of the shear planes. The factors affecting aggregate interlock are discussed in section 5.7.

6.2.3 Shear transfer by dowel action of bonded reinforcement and prestress tendons (if provided)  $F_d$ : At present, the amount of published work on dowel action is very limited and there is no general theory to evaluate its effect on the shear carrying capacity of concrete structures. The dowel forces can be influenced by the tensile strength of the concrete, bar size and spacing, concrete cover and length of bar and the width of the cracks where the shear displacement occurs. The shear resistance produced by small percentages of reinforcement in end slabs was found to be very small (see section 5.8).

### 6.3 Simplified Methods of Analysis

6.3.1 Principal tensile stress approach: In this method the proportion of hoop prestress above a horizontal line through the limit of the haunch crack is assumed to produce a uniform radial compression along the inclined failure plane. The position of the haunch crack and the failure plane may be taken from experimental observations.

By relating the shear and radial stress it was found that in the "C" series of models, the principal plane coincided with the observed angle of the failure plane. Thus, by assuming a limiting value for the principal tensile stress it was possible to determine an average shear stress capacity for the slab section. This shear stress was assumed to act on a cylindrical surface with a radius equal to the mean value for the truncated conical plug. Assuming a value for the principal tensile stress of  $0.1 f_c'$  which is a mean value of the modulus of rupture and direct tensile strength, a failing pressure was then derived. A comparison of predicted and actual failing pressures is given in Table 6.1, column 8. The principal tensile stress approach assumes that the shear strength increases with the lateral restraint. Higher theoretical ultimate pressures should therefore be obtained if the lateral prestress is increased; this is not however in agreement with experimental results.

Campbell-Allen has developed a method for determining the ultimate strength of thick slabs. This is based on a Mohr failure envelope which defines the interrelationship between the normal and tangential stresses on the failure surface. The Mohr envelope is valid for concrete subject to triaxial compression, however, it was assumed that the theory could be linearly extrapolated for the tension zone. The lower bound solution over estimates the failing pressure by at least 50%.

Both methods over simplify the failure mechanism actually occurring and it would appear that the simple criteria adopted are not appropriate.

6.3.2 Nominal shear stress or empirical approach: Although the problem of shear in thick restrained slabs is complicated due to the nature of the stresses developing within the concrete, it has been found that the average shear stress at ultimate can be related to the

uniaxial compressive strength of the concrete.

For comparative purposes the ultimate shear stress was calculated at the junction between the slab and the extension of the barrel. The average shear stress ranged between 16 and 25  $\sqrt{f'_c}$  (see Table 6.1, column 6).

Another approach was made to obtain an analytical expression which would give better correlation with the available results and which takes into consideration the effect of the lateral prestress, depth to span ratio as well as the strength of the concrete. The following empirical relationship was found for the ultimate pressure :

$$P = 77 \frac{d}{D} \sqrt{f'_c} + 10 \left(1 - \frac{D}{\phi}\right)^{\frac{1}{2}} \sqrt{f_h} \dots\dots (1)$$

where P = ultimate pressure in lb/sq.in.

$f_h$  = average compressive stress from the lateral prestress in lb/sq.in.

A comparison of the results obtained using this equation with the test data is given in Table 6.1, column 9. Values of  $P_{theor.}/P_{expt.}$  ranged from 0.82 to 1.34 with a coefficient of variation of 15%.

This equation is based on a small number of tests and can only be considered to be applicable to structural members similar to the test slabs. With additional data a more generally applicable expression similar to the above could be developed.

6.3.3 Approach based on mode of failure: The assumption of uniform stress across the section adopted in the principal tensile stress approach is invalid. From typical measurements of strains in a number of pile caps the maximum compression was in the region of 6000 with tensile values of 8000 microstrain. Fig.19 shows the change in the zone of tensile strain with increasing pressure. As stated approximately 15% of the depth was in compression at failure.

- a. Shear Resistance of Tensile Zone. The resistance can be assumed to be generated by the vertical component of the aggregate interlock or failure can be calculated on the basis of a limiting principal tension where the field stress is already tensile.

In Fenwick's work the aggregate interlock was determined for a minimum crack width of .0075 in. (0.19 mm). In the experimental work described the crack widths just prior to failure were derived by subtracting a value for the elastic strain, based on a linear extension, from the total radial deformation of the slab. The calculated crack widths were about .003 in. (0.08 mm) and therefore a value for the aggregate interlock was found by extrapolation.

- b. Shear Resistance of the Compression Zone. This can be assessed on the basis of a limiting value for the principal tensile stress; the biaxial compression is directly derived from the hoop prestress force above the tip of the haunch crack. If a value of 400 lb/sq.in. is adopted for the principal tensile stress then the resistance of the compression zone is 25% of the total shear force. This stress is an accepted value for the design of conventional structures. The latest British Draft Code of Practice for the structural use of concrete allows a principal tensile stress of approximately  $0.1 f'_c$  for the design of anchorage

zones in prestressed concrete members for the limit state of local damage. If this higher value were used the shear resistance would approach 45% of the total shear force. Alternatively, the shear resistance can be abstracted from the authors' experimental work on deep elements failing in shear compression (Fig.20). Using this information the shear resistance of the compression zone was 45% of the total.

## 7. CONCLUSIONS

- 7.1 In relation to the other fields of structural research only a limited amount of experimental work has been completed on the shear compression failure of pile caps or deep restrained circular slabs. In common with other structural elements where shear predominates, a full understanding of the mechanism of failure has still to be developed.
- 7.2 To establish a theory which will describe the types of collapse observed experimentally, considerable further study is required to determine the criteria of failure of concrete under the complex stress states and restraints that exist in a pile cap.
- 7.3 In the interim, simplified approaches similar to those used for conventional structural elements may be used to predict a lower bound value for the ultimate strength. Empirical approaches can thus be used for dimensioning the pile cap provided the geometry and penetration arrays are comparable with the various models described in this paper. The designer must still rely on a model investigation for final confirmation of the reserve of strength as the basis for any empirical method is not yet sufficiently confirmed.
- 7.4 The effects of the major parameters on the ultimate strength may be summarised :
- a. An increase in the thickness of the slab in relation to its span has a dominant effect on the ultimate strength.
  - b. Provision of hoop prestress or lateral restraint increases the ultimate strength of the slab but the rate of increase of strength progressively falls. At the magnitude of prestress required for producing acceptable stress levels under reactor working conditions the ultimate strength is not significantly affected by variation of the hoop prestress.
  - c. Variations of boundary conditions within the limits described in the paper do not appear to significantly affect the failing pressure.
  - d. When penetrations are incorporated in the slab the liners partly compensate, by dowel action, for the loss of the area of concrete acting in shear. The loss of strength due to the introduction of a standpipe array is therefore not severe.
  - e. For similar shapes of pile cap the ultimate shear strength has been found to be approximately proportional to the square root of the cylinder strength of the concrete; reinforcement in the quantities conventionally used has little effect.

## REFERENCES

1. Brading, K. F. and Hills, G., "Use of Structural Models in Developing Pressure Vessel Design". Proceedings of Conference on Prestressed Concrete Pressure Vessels, Institution of Civil Engineers, London 1968.

2. Campbell-Allen, D. and Low, E. W. E., Pressure Tests on End Slabs for Prestressed Concrete Pressure Vessels, Nuclear Engineering and Design, 1967, Vol.6, No.4.
3. Morgan, P. L. T., "Discussion, Proceedings of Conference on Prestressed Concrete Pressure Vessels, Institution of Civil Engineers, London 1968.
4. Campbell-Allen, D. and Low, E. W. E., "The Use of Simplified Models for the Design of End Slabs", Proceedings of Conference on Model Techniques for Prestressed Concrete Pressure Vessels, British Nuclear Energy Society, London 1969.
5. Paul, S. L., Sozen, M. A., Schnobrich, W. C., Karlsson, B. I. and Zimmer, A., "Strength and Behaviour of Prestressed Concrete Vessels for Nuclear Reactors", Civil Engineering Studies, Structural Research Series No. 346, University of Illinois, July 1969.
6. Meerwald, K. and Schwierts, G., "Testing of a Perforated Prestressed Concrete Pressure Vessel Top Slab Model", American Concrete Institute Seminar on Concrete for Nuclear Reactors, Berlin, October 1970.
7. Garas, F. K., "Discussion of Symposiums on Model Technique for Prestressed Concrete Pressure Vessels", British Nuclear Energy Society, London 1969.
8. Langan, D., O'Flynn, M. C. and Welch, A. K., "The Design of Pod Boiler Pressure Vessels with Particular Reference to Hartlepool Nuclear Power Station", Paper HA/4, First International Conference on Structural Mechanics in Reactor Technology, Berlin, September 1971.
9. Proceedings of Conference on Prestressed Concrete Pressure Vessels, Institution of Civil Engineers, London 1968.
10. Symposium on Model Technique for Prestressed Concrete Pressure Vessels, British Nuclear Energy Society, London 1969.
11. Garas, F. K. and Langan, D., "The Capacity of Prestressed Concrete Pressure Vessel Components to Resist Shear", American Concrete Institute Seminar on Concrete for Nuclear Reactors, Berlin, October 1970, to be published.
12. Moe, J., "Shearing Strength of Reinforced Concrete Slabs and Footings under Concentrated Loads", Bulletin D47, Portland Cement Association, Research & Development Laboratories, 1961.
13. Langan, D. and Garas, F. K., "The Failure of Concrete under the Combined Action of High Shearing Forces and Biaxial Restraint", International Conference on Structure, Solid Mechanics and Engineering Design in Civil Engineering Materials, Southampton, April 1969.
14. Smee, D. J., "The Effect of Aggregate Size and Concrete Strength on the Failure of Concrete under Triaxial Compression", Civil Engineering Transactions, October 1967.
15. Fenwick, R. C. and Paulay Thomas, "Mechanism of Shear Resistance of Concrete Beams". Journal of the Structural Division, Proceedings of the American Society of Civil Engineers, October 1968.
16. Thanlow, S., "Tensile Splitting Test and High Strength Concrete Test Cylinders". Journal of American Concrete Institute, V53 January 1957.
17. Elstner, R. C. and Hognested, E., "Shearing Strength of Reinforced Concrete Slabs",

Journal of the American Concrete Institute, Vol.53, No.1, July 1956.

18. Billig, K., Structural Concrete, Macmillan & Co. Ltd., London 1963, P.136.

ACKNOWLEDGEMENTS

The authors wish to thank Taylor Woodrow Construction Ltd. for permission to publish this paper and also to their colleagues for their contribution.

TABLE 4.1 - TEST PROGRAMME AND MODES OF FAILURE

Slab No.	Percentage Reinforcement	Stand-pipes	Wall Penetrations	Vertical Prestress lb/sq.in.*	Hoop Prestress lb/sq.in.	Crushing Strength lb/sq.in.	Mode of Failure
(1)	(2)	(3)	(4)	(5)	(6)	(7)	(8)
D1	0.44	Yes	No	2100	600	7250	P
D2	0.44	Yes	No	2100	600	7750	P
C1	0.44	No	No	2760	600	7950	S
C2	0.44	No	No	2760	600	7750	S
C3	0.44	Yes	No	920	600	9050	S
C4	0.44	Yes	No	2760	600	8500	S
C5	No	Yes	No	2760	600	6600	S
C6	No	No	No	2760	600	7750	P
C7	0.44	Yes	Yes	2760	600	7750	S
C8	0.44	Yes	Yes	920	600	6150	S
C9	0.44	Yes	No	2760	600	9200	S
		(unlined)					
C10	0.44	Yes	Yes	2760	600	10350	S
C11	0.44	No	No	2760	600	6750	S
C12	0.44	No	No	2760	360	5800	S
C13	0.44	No	No	2760	No	8750	S
C14	0.44	No	No	2760	600	3050	S
C15	0.64	No	No	2760	600	Under test	
G1	0.92	Yes	No	845/2480	880	9150	S
G2	0.92	Yes	No	845/2480	660	9000	S
M0	No	Yes	Yes	2100	900	9700	S
M1	No	Yes	Yes	2100	900	Under test	
M2	No	Yes	Yes	2100	900	Under test	
M3	No	Yes	Yes	2100	900	Under test	

Notes :

\* 145 lb/sq.in. = 1N/mm<sup>2</sup>

Col. 5. Vertical prestress - all figures are equivalent internal pressure.

Col. 7. Crushing strength was determined from 4 in. cubes.

Col. 8. Modes of failure : P - Hoop prestress, S - Shear.

TABLE 6.1 - SUMMARY OF EXPERIMENTAL AND THEORETICAL RESULTS

AUTHORITY	SLAB NO.	d/D	f' <sub>c</sub>	f <sub>h</sub>	$\frac{\tau_{\text{expt.}}}{\sqrt{f'_c}}$	P <sub>expt.</sub>	$\frac{P_{\text{theor.1}}}{P_{\text{expt.}}}$	$\frac{P_{\text{theor.2}}}{P_{\text{expt.}}}$
(1)	(2)	(3)	(4)	(5)	(6)	(7)	(8)	(9)
Authors	C1	0.40	7550	600	21.6	3000	0.95	0.95
	CM	0.40	7600	600	19.4	2700	1.06	1.06
	C12	0.40	5500	360	21.1	2500	0.81	0.97
	C14	0.40	2900	600	25.0	2150	0.59	0.85
	MO	0.46	9500	900	21.8	3900	1.04	0.95
	G1	0.49	8700	880	24.6	4500	0.83	0.82
	G2	0.49	8600	660	22.5	4100	0.88	0.89
Campbell-Allen	I	0.27	9150	1300	15.9	1640	1.15	1.34
	II	0.27	8850	1850	16.4	1670	1.20	1.33
	III	0.27	8050	3500	18.7	1805	1.28	1.19
	IV	0.27	8100	2150	22.3	2170	0.91	0.99
	V	0.55	8050	2680	20.1	3950	1.25	1.04
	VI	0.55	8800	1210	19.3	3985	1.15	1.05
Illinois	PV15	0.30	7340	1300	22.4	2300	0.78	0.96
	PV16	0.40	7450	1210	23.2	3200	0.80	0.90
	PV17	0.40	7180	1270	22.2	3000	0.84	0.94
	PV18	0.40	7590	1190	21.6	3000	0.86	0.96
	PV19	0.40	7470	1170	25.4	3500	0.80	0.82
	PV20	0.40	6890	1150	24.9	3300	0.72	0.84
	PV21	0.40	7400	1130	24.0	3300	0.76	0.87
						<u>Mean</u>	0.93	0.99

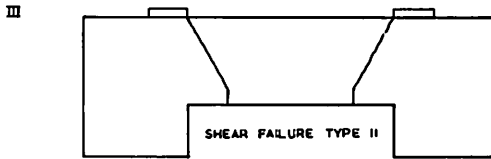
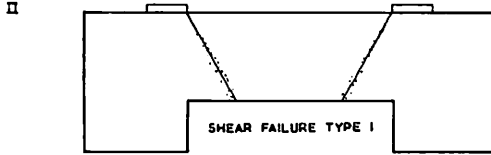
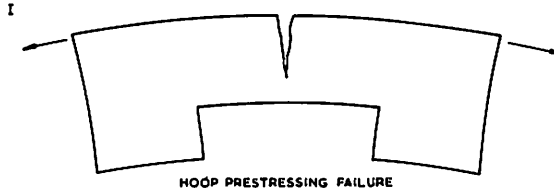
Notes: Col.2. CM Typical slab of the C Series.

Col.6.  $\tau_{\text{expt.}}$  - ultimate shear stress calculated at the junction between the slab and the extension of the barrel.

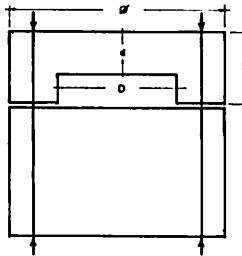
Col.8.  $P_{\text{theor.1}}$  - calculated ultimate pressure using the principal tensile stress method.

Col.9.  $P_{\text{theor.2}}$  - calculated ultimate pressure using equation 1.

Coefficient of Variation 20% 15%



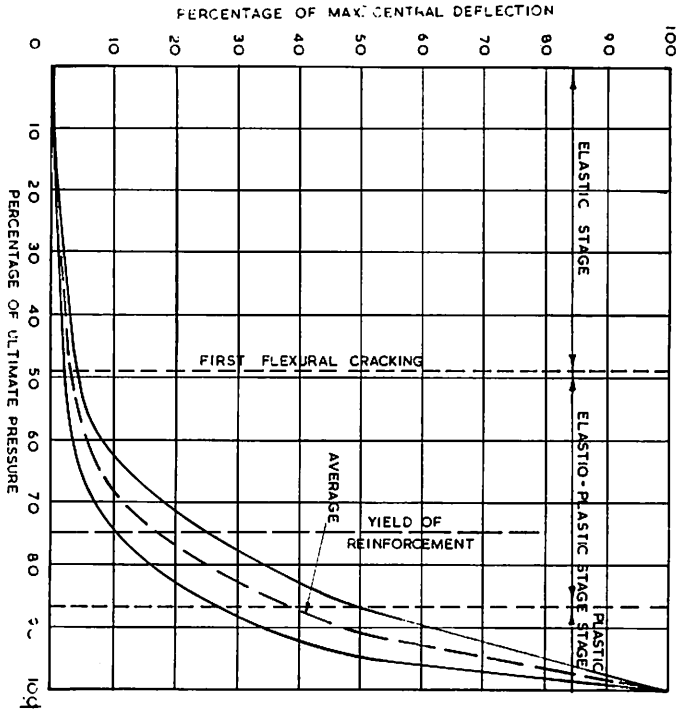
1. Possible Modes of Failure



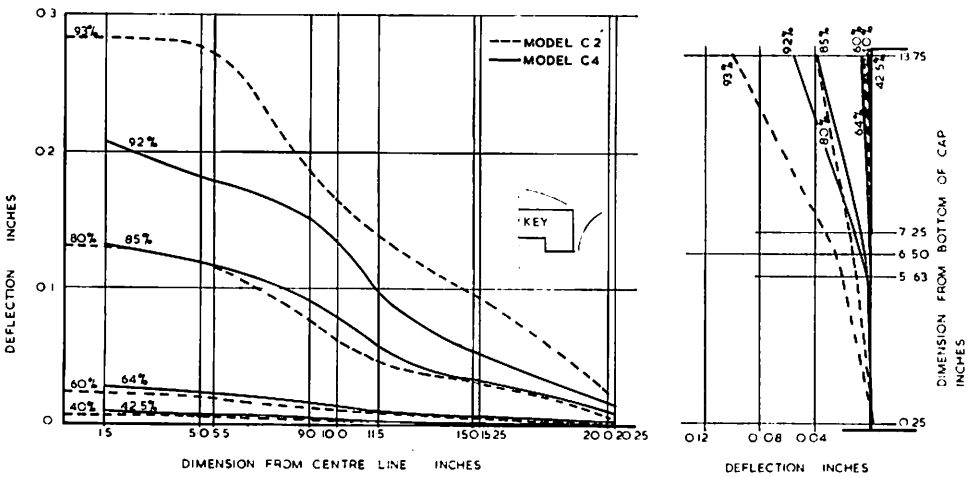
SLAB No.	DIMENSIONS (INCHES)				WIRE USED FOR HOOP PRESTRESSING	
	$\sigma$	D	d	h	DIAMETER OF HOOP PRESTRESSING WIRE (INCHES)	ULTIMATE TENSILE STRENGTH (TONS. F/INCH <sup>2</sup> )
D.1	43.25	22.25	9.0	9.0	0.036	150 - 160
D.2	43.25	22.25	9.0	9.0	0.036	150 - 160
C.1	43.25	22.25	9.0	14.0	0.036	150 - 160
C.15	43.25	22.25	7.5	12.5	0.036	150 - 160
G1 & G2	45.25	28.73	14.20	29.0	0.250	100 - 110
M.O	42.875	17.50	8.125	12.50	0.036	150 - 160
M1 & M2	128.625	52.50	24.50	37.50	0.104	120 - 130
M.3	125.00	52.50	23.94	36.94	0.104	120 - 130

1 ton = 2240 lbs  
 1 inch = 25.4 mm

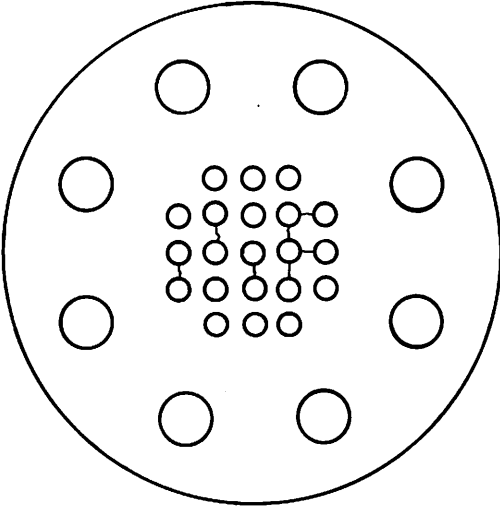
2. Experimental Details



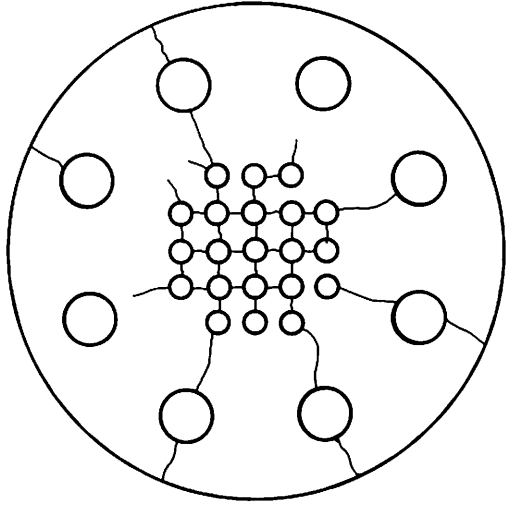
3. Flexural Behaviour



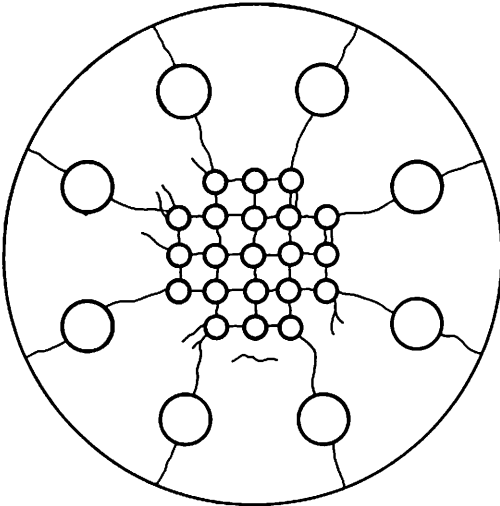
4. Typical Deflected Profiles for Perforated and Unperforated Caps



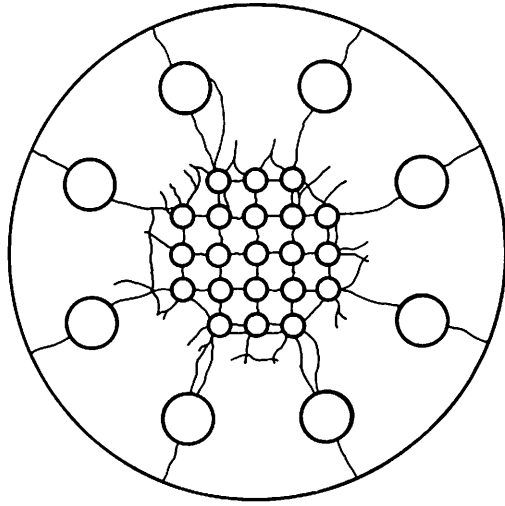
59% OF ULTIMATE  
PRESSURE



71% OF ULTIMATE  
PRESSURE

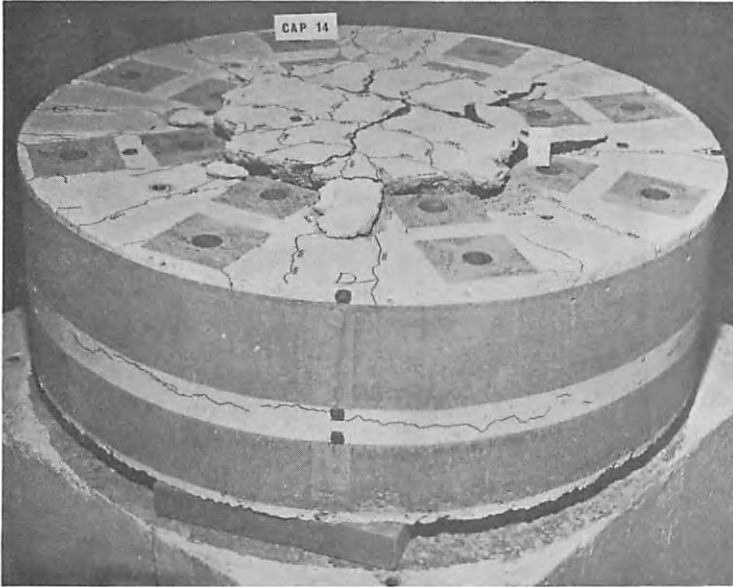


93% OF ULTIMATE  
PRESSURE

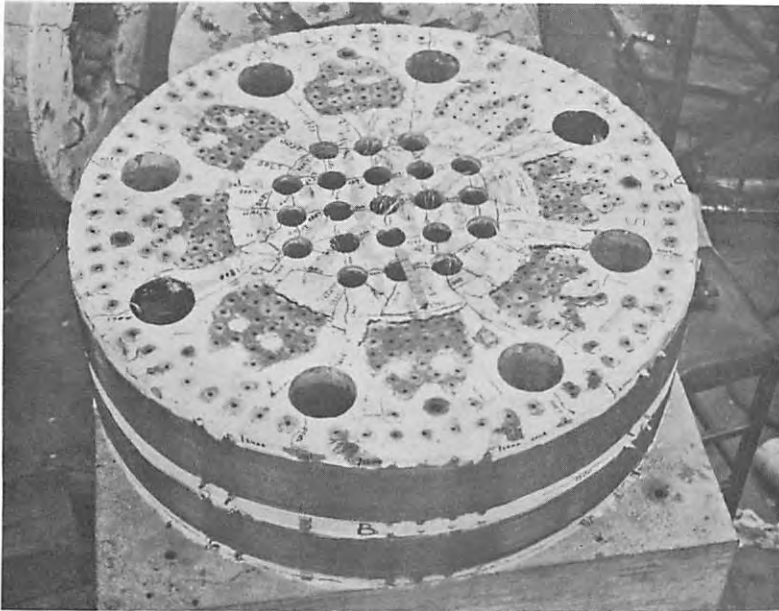


AT FAILURE

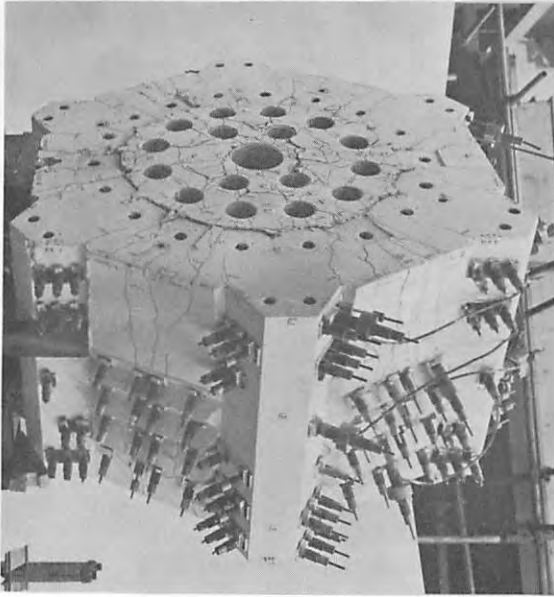
5. Crack Propagation



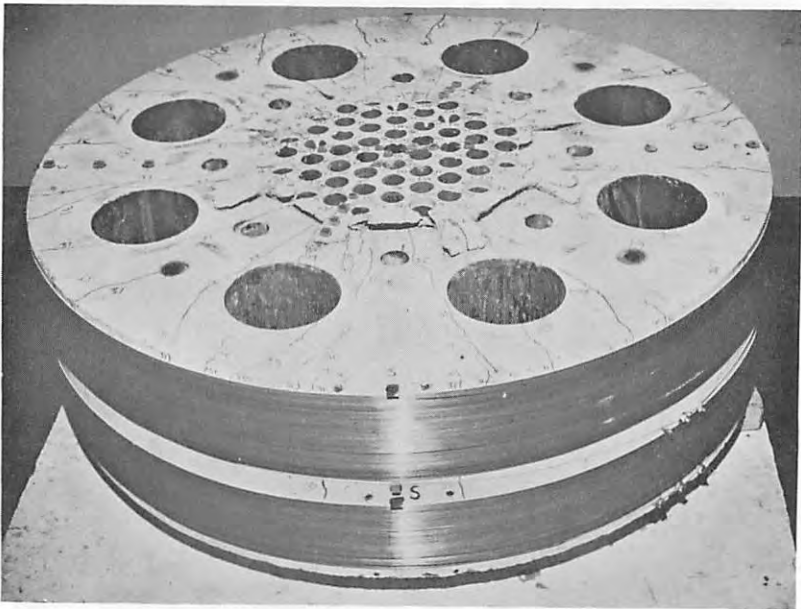
6. Failure of Unperforated Cap (Model C14)



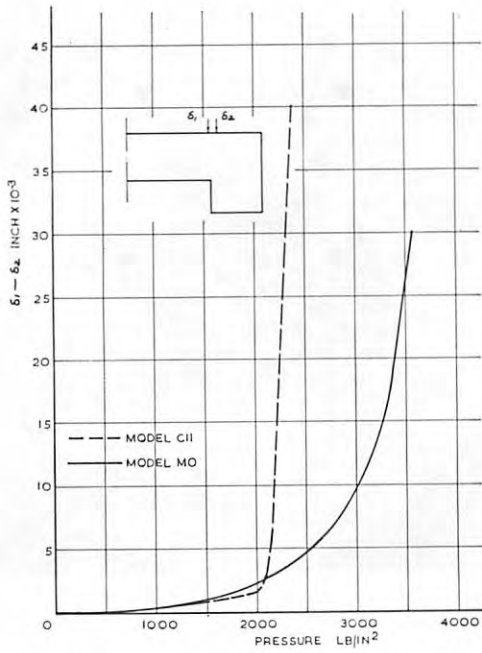
7. Failure of Perforated Cap (Model C10)



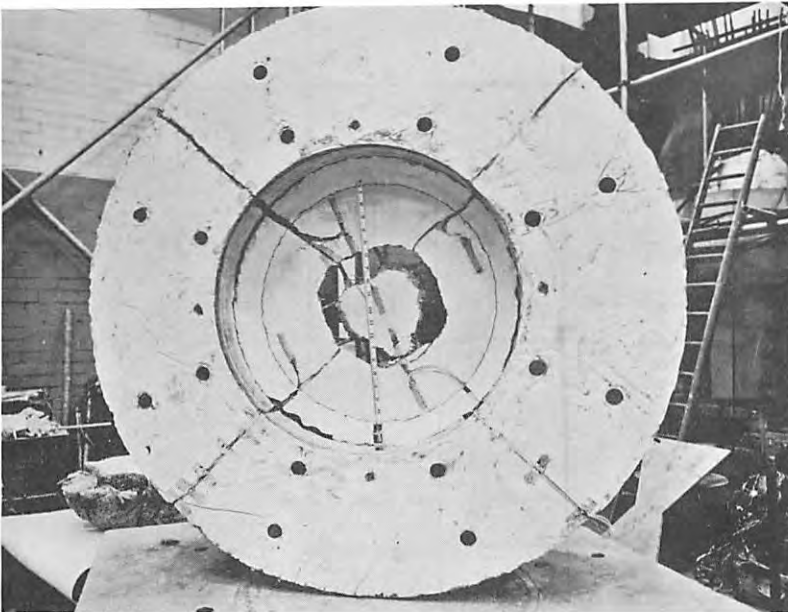
8. Failure of Fort St. Vrain Head (Model G1)



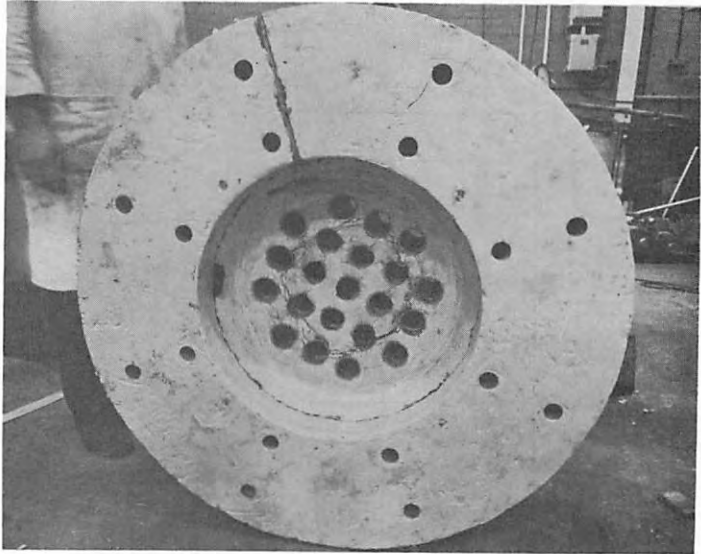
9. Failure of Perforated Cap (Model M0)



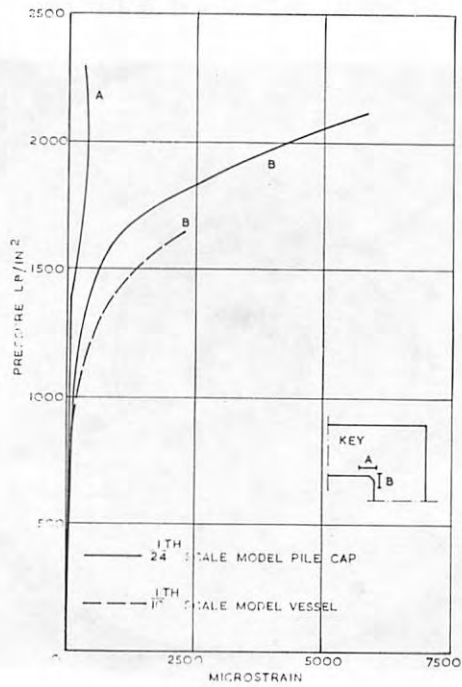
10. Differential Deflection at Failure Plane



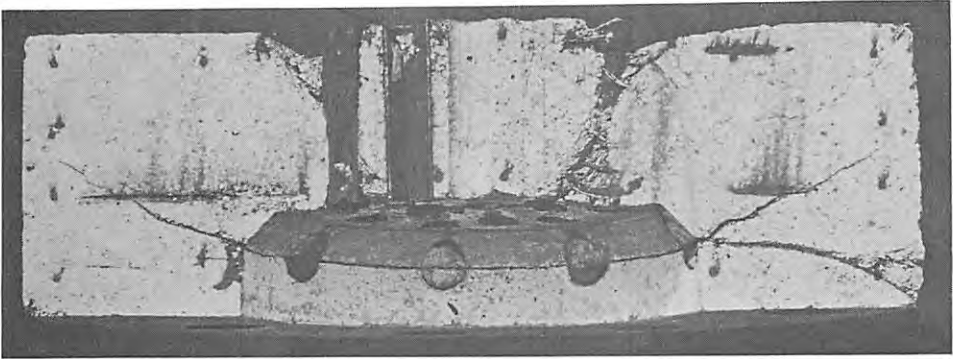
11. Inside View of Unperforated Model



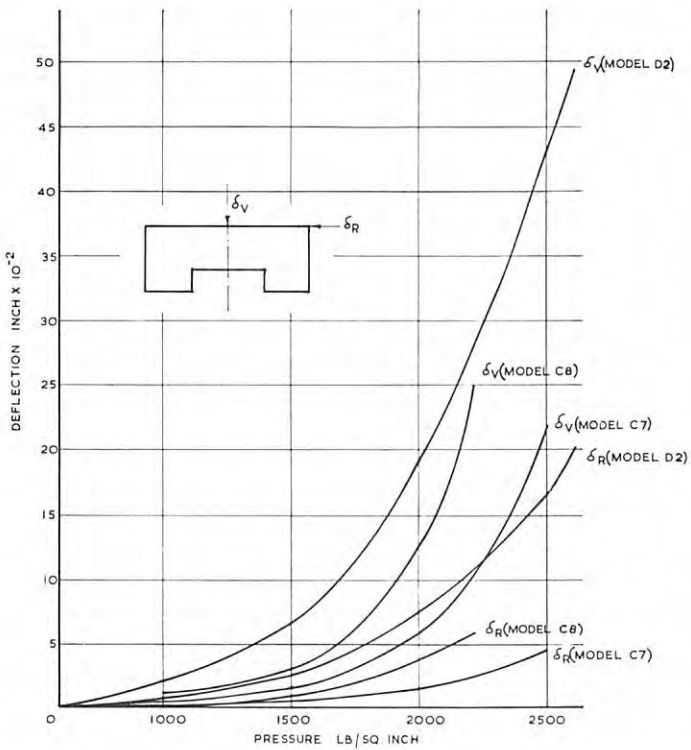
12. Inside View of Perforated Model



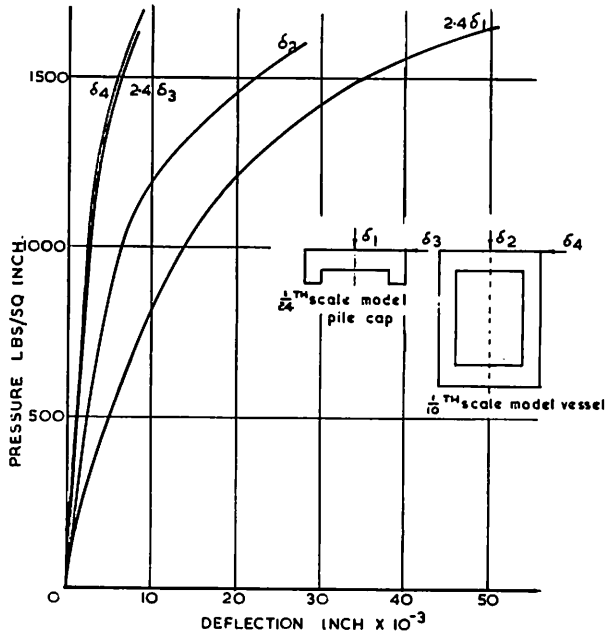
13. Strains at Haunch



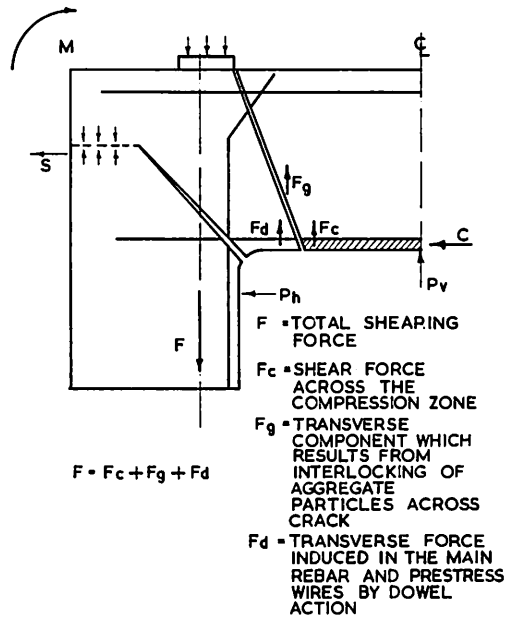
14. Cross Section of Model C8 After Failure



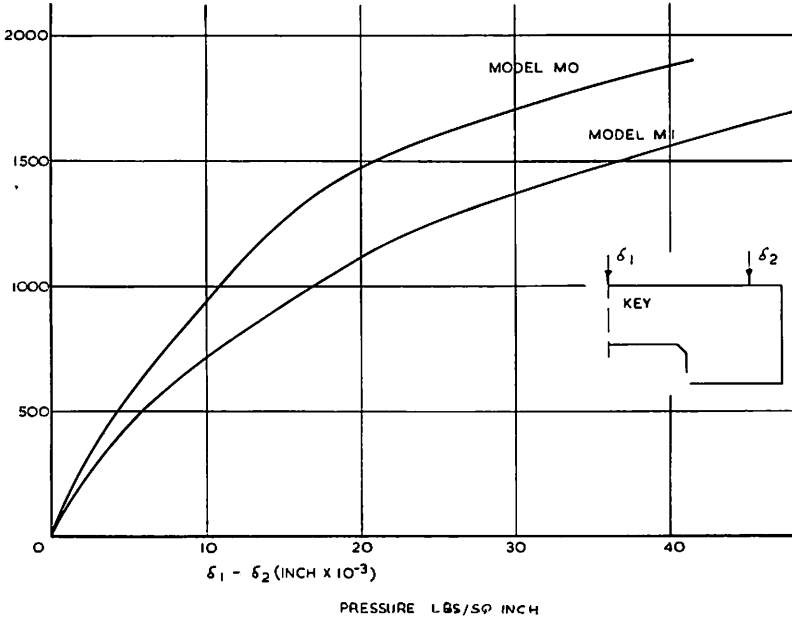
15. Effect of Boundary Conditions on Central and Radial Deflections



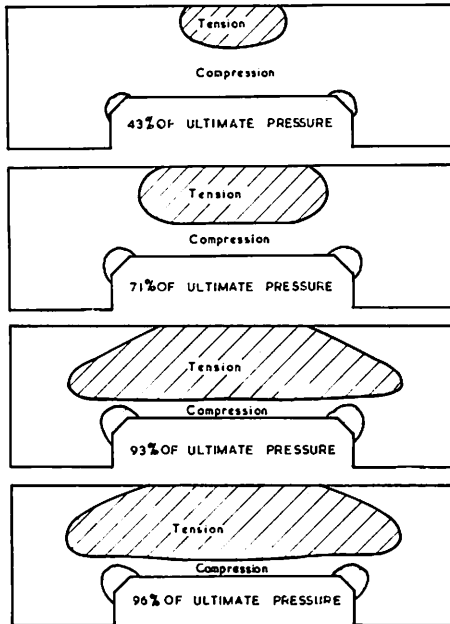
16. Comparison of Deflections for Complete Model and Isolated Cap



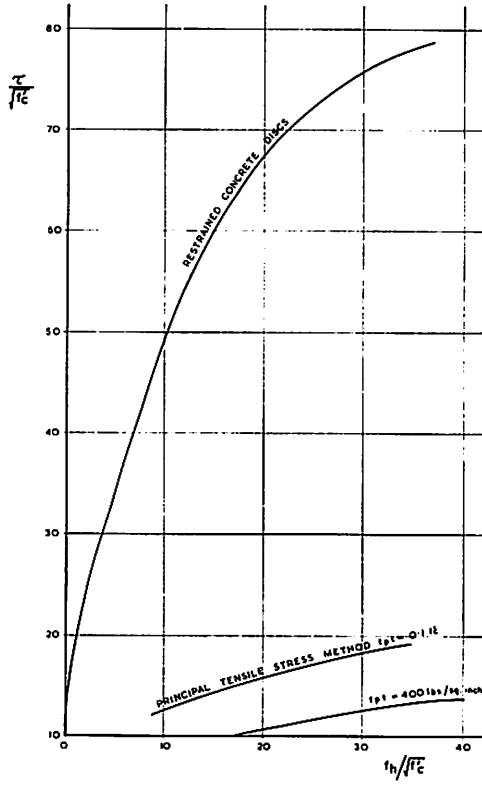
17 Mechanism of Shear Failure



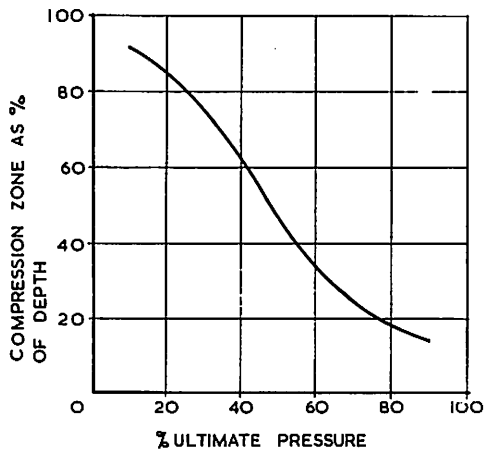
18. Effect of Model Scale on Central Deflections



19. Development of Zones of Tensile Stress



20. Relationship of Shear Stress to Biaxial Compression



21. Reduction of Depth of Compression Zone with Pressure

C G. D. STEFANO, U. K.

Elastic and ultimate tests of a prestressed concrete pressure vessel model.

### 1. Introduction

I am very much interested in the behaviour of end slabs in cylindrical reactor pressure vessels and the experimental work presented by the authors of paper H 3/4.

Although the work of the authors concerns itself mainly with the mode of failure and the behaviour of deep prestressed circular slabs, the work which I am going to report considers the behaviour of a cylindrical reactor vessel model, prestressed longitudinally and circumferentially and subjected to an internal pressure. The model was designed and constructed in the structure laboratory of the City University London, as a research project for students in the Department of Civil Engineering. A general view of the vessel and test rigs is shown in Fig. 1.

The aim of the project was :

- a) to observe the elastic behaviour of the model under working load conditions;
- b) to see whether the distribution of strain in the vessel for the working load would indicate the probable mode of failure, and
- c) to verify the above by loading the vessel to failure.

### 2. Vessel Specification and Materials

The model shown in Fig. 2 was built to a scale of approximately 1/50 and had the following dimensions :

Overall height	3 ft.
External diameter	1 ft. 11 in.
Internal diameter	1 ft. 3 in.
Wall thickness	4 in.
End slab thickness	6 in.

The concrete mix proportions were 1:1.65:2.19, cement : sand : aggregate (3/8" max. size) and the W/C ratio 0.46. The compressive strength of the mix at 28 days was 6900psi. The tensile strength was 430psi. and its modulus of elasticity  $6.13 \times 10^6$  psi. Post-tensioned prestressing wire was used throughout with an elastic modulus of  $29 \times 10^6$  psi. The vessel was not reinforced with mild steel and thin copper sheeting was used for lining. Fig. 3.

### 3. Design Criteria

The model was designed according to the design criteria used in current practice with respect to elastic respond at operating loads, the mode of failure to be gradual and a specified ultimate load factor. Fig. 4 shows the estimated pressures for various modes of failure.

### 4. Elastic Testing

The vessel was tested in the range 0 to 300 psi. and readings were taken at increments of 50 psi. Throughout the testing the vessel showed no signs of cracking. The deflections recorded during the test in the end caps and the walls were of the form that would be expected. The strains, however, showed some interesting features.

Fig. 5 shows a definite weak point in the structure between Demec gauge points 16 and 17 and above 300 psi. pressure the strains along the circumference are in excess of the calculated  $19.7 \times 10^{-5}$ . Fig. 6 shows another weak point at G and this is the same point at which the high circumferential strains occurred, Fig. 7.

#### 5. Ultimate Load Test

After the elastic tests had been completed the pressure in the vessel was raised in 100 psi. increments. Failure occurred when the pressure reached the value of 550 psi. . The experimental results were plotted and are shown in Figs. 7 and 8.

#### 6. Discussion of Results

From the results it was clearly seen that the model failed at an applied pressure of 550 psi. . It showed a progressive mode of failure giving adequate warning of impending failure. The failure of the vessel occurred with three large vertical cracks and four small circumferential as shown in Figs. 9 and 10 and 11. The vertical cracks followed the line of vertical tendons and the lateral cracks followed the construction joints. Fig. 9.

The top cap also cracked in two, roughly on a diameter as shown in Fig. 12. The tests confirmed that the predicted mode of failure compared well with the actual mode of failure. The predictions indicated that the vessel would fail by vertical cracking at an applied pressure of 427 psi. . Cracking actually occurred between 400 and 550 psi.

Circumferential cracking was not expected until much higher pressures were reached. However, these cracks were formed along construction joints, which must have been weaker than other sections of the vessel. Moreover, the large amount of vertical cracking would have produced shear stresses to develop along these places of weakness.

One point which became clear from the ultimate load test is that these vessels require some form of mild reinforcement. Mild steel would have increased the ultimate failure load and it would further guarantee a progressive mode of failure.

The results from this pilot test could only give qualitative indications of the vessels behaviour. For more positive conclusions more detailed models would be necessary. Nevertheless, the crack pattern of the end cap appears to be different from those observed by the authors of paper H 3/4.

I would appreciate, therefore, if the authors would like to comment on my preliminary observations and findings. Perhaps they would also like to indicate the possible effects on the mode of failure due to temperature and sustained loading.

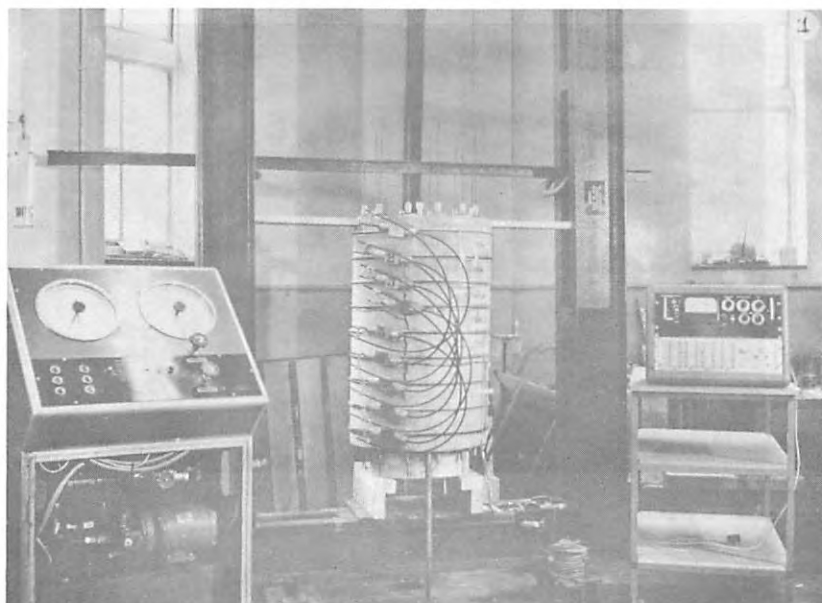


Fig. 1

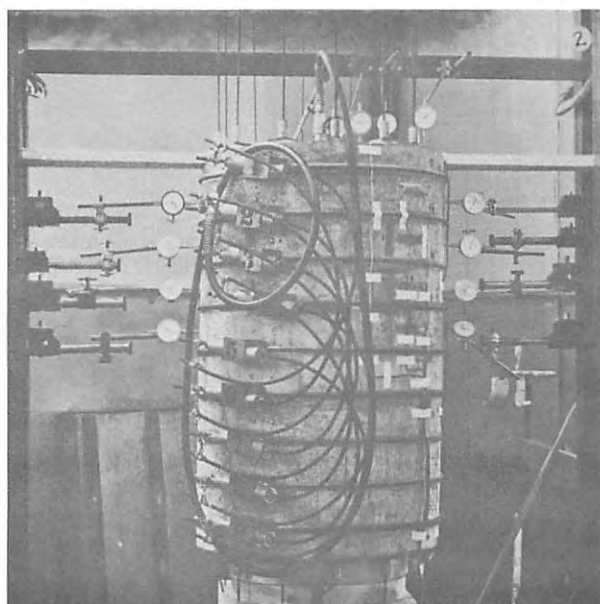


Fig. 2

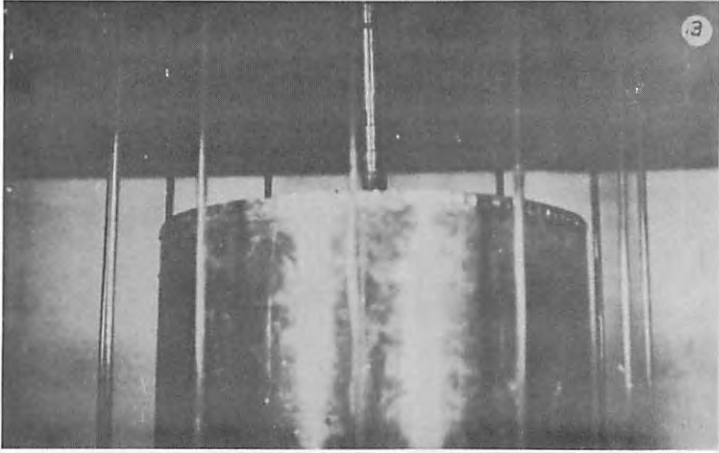


Fig. 3

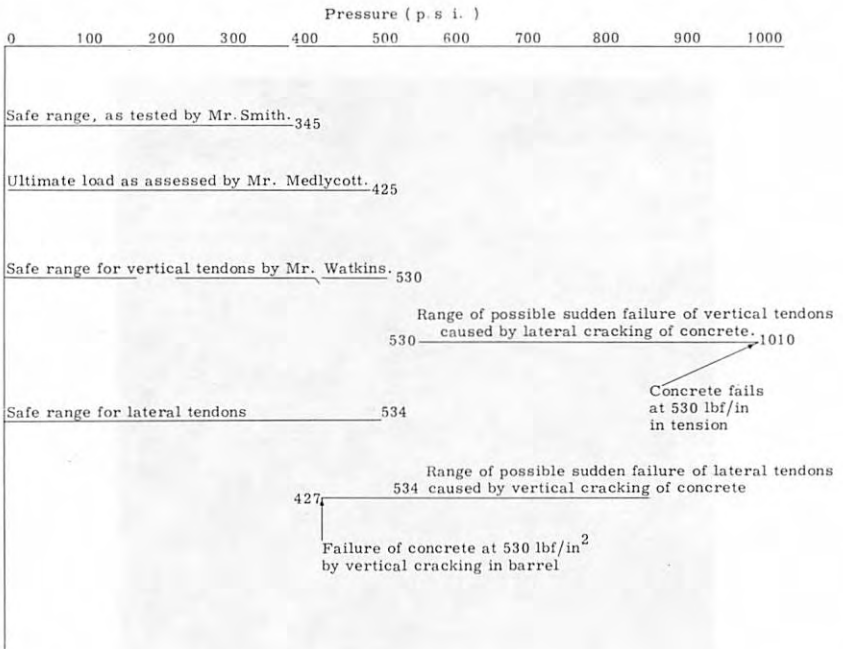


Fig. 4 ESTIMATED PRESSURES FOR VARIOUS MODES OF FAILURE.

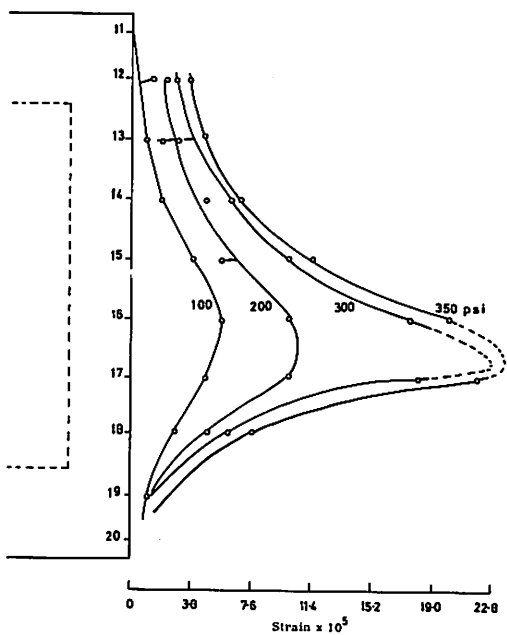


Fig. 5 CIRCUMFERENTIAL STRAINS ( DEMEC GAUGE READINGS )

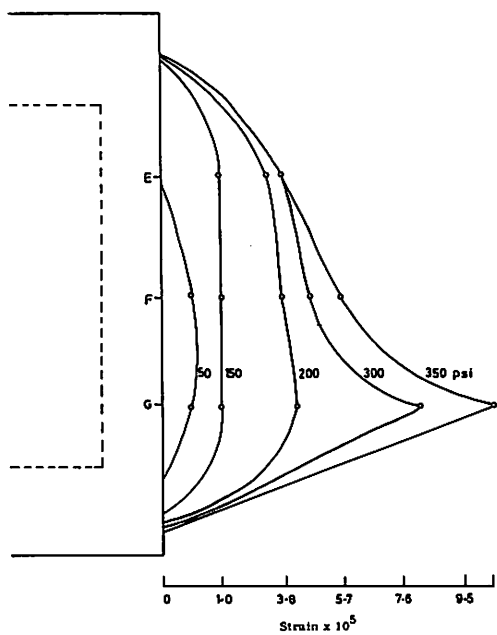


Fig. 6 LONGITUDINAL STRAINS ( DEMEC GAUGE READINGS )

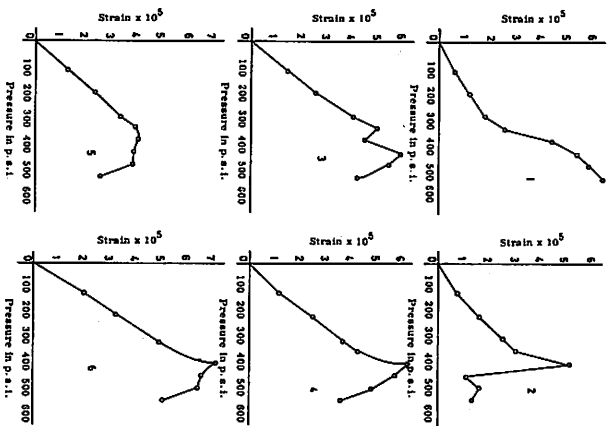


Fig. 7 ULTIMATE LOAD TEST : GRAPHS FOR INDIVIDUAL E. R. S. GAUGES

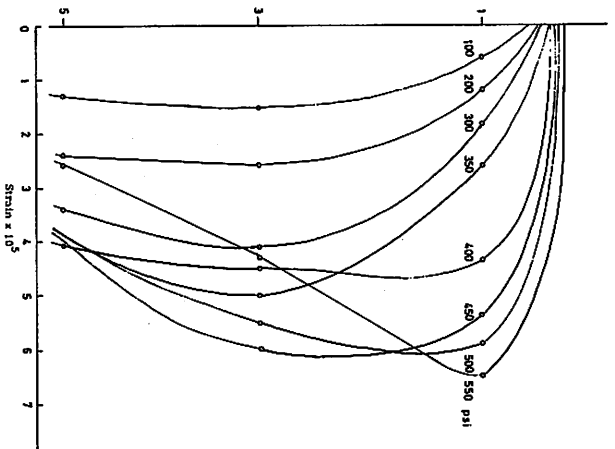


Fig. 8 ENLARGEMENT OF ( LONGITUDINAL STRAINS )

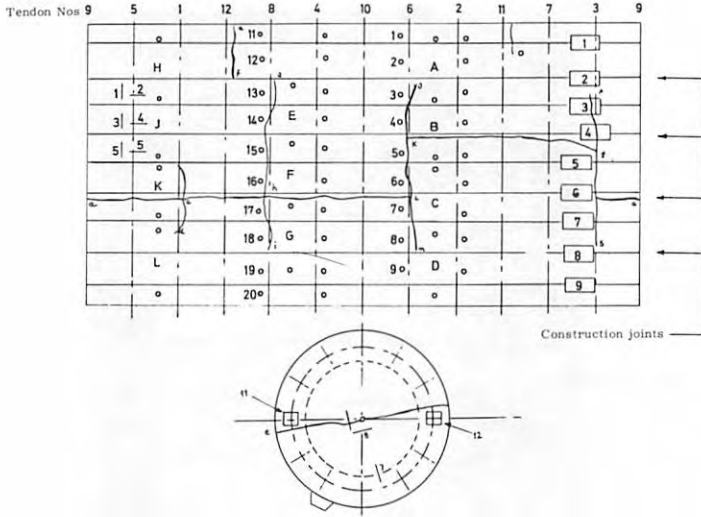


Fig. 9 CRACK POSITIONS AFTER ULTIMATE LOAD TEST



Fig. 10

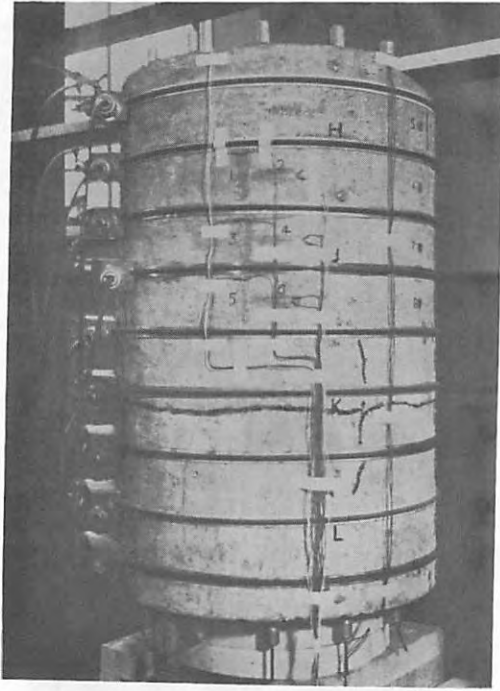


Fig. 11

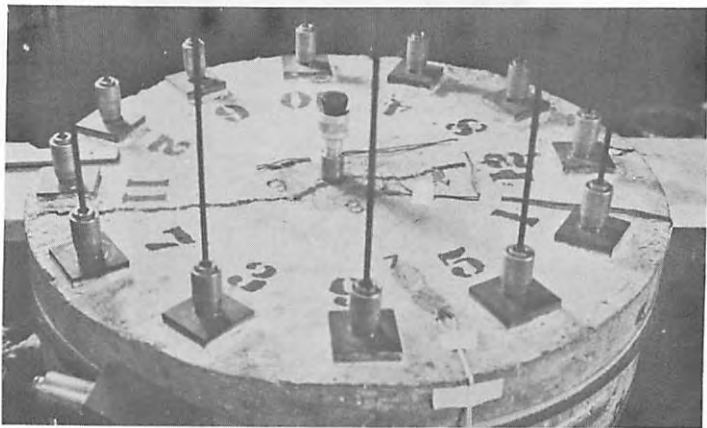


Fig. 12

F. K. GARAS, U. K.

C

The end slab or closure is generally subject to a temperature gradient. This may cause degradation of the concrete in the Standpipe zone. The effect of degradation has been simulated in our work by testing a model with a low concrete strength. Comparison between models C11 and C14 (reference paper H 3/4) shows a reduction of 28% in the failure pressure. Figs. 1 and 2 show the effect of concrete strength on the central deflection and shear deformation of models C11 and C14. The difference in behaviour is obviously due to the difference in the modulus of elasticity.

The effect of concrete strength on the shearing resistance was also examined in our work on small elements; Fig. 3 (reference 1).

By comparing the results obtained from three different concretes with cylinder strength of 2,300, 6,400 and 10,700 lb/sq. in. the reduction in concrete strength lowered the shearing strength by an amount which was proportional to the square root of the ratio of the concrete strength.

Another parameter which we examined is the effect of penetrations. It has been found that the presence of penetrations had little effect on the failing pressure. However, it was found that the orientation of the stand tubes had influence on the mode of failure. Fig. 4 shows a cross section of model MO after failure. The central plug sheared at an angle of 35° to the vertical on the line of the anchor plates and 60° to the vertical between the anchor plates. These cracks extended two inches below the top of the cap where they reached the standpipe zone. Here the central plug sheared along the concrete-steel interface of the outer array of standpipes. This mode of failure was certainly different for models of the C series as shown in Fig. 14 of the paper.

Fig. 5 shows the central deflection of two models C11 and C13. C11 had a hoop prestress of 600 lb/sq. in. whilst C13 had no restraint at all. The failure of C11 was a sudden shear type failure whilst that of C13 was progressive.

The possibility of applying beam theory to slabs has been considered in our work on shear in an attempt to understand the failure mechanism of end slabs. A number of restrained beams having a span to depth ratio of 2.5, similar to the C series were loaded under different degrees of restraint.

Fig. 6 shows the experimental arrangement which was used. The lateral restraint was applied externally by the use of 4 no. Lee McCall bars. The beam was clamped to a base slab by means of 4 no. Lee McCall bars and a rubber chamber was used to produce water pressure and acted as a liner between the beam and the test base.

The results in Fig. 7 indicate that an increase in the restraint from zero to 6%  $f_c$  is the cylinder compressive strength. This is due to a change from flexural failure to a jammed shear compression failure caused by the compressive membrane action. A further increase of restraint to 24%  $f_c$  only produced an additional 19% in the shear strength.

Table 1 gives an appreciation of the magnitude of the nominal shear stresses which may develop in conventional and deep beams and slabs. From these data it can be seen that the nominal shear stresses which develop in deep beams and slabs are very similar. For design consideration an average nominal shear stress equivalent to  $18\sqrt{f_c}$  can be assured for end

slab of prestressed concrete pressure vessels.

Table 1 - Nominal Shear Stresses in Beams and Slabs as a Function of Compressive Cylinder Strength

Type of Element	Nominal Shear Stresses
Conventional Unrestrained Beams	$2 - 4 \sqrt{f_c}$
Conventional Unrestrained Slabs	$6 - 9 \sqrt{f_c}$
Restrained Deep Beams (span/depth ratio = 2.5)	$16 - 19 \sqrt{f_c}$
Restrained Deep Slabs (span/depth ratio = 1.8 to 3.7)	$16 - 24 \sqrt{f_c}$

Reference:

- (1) D. Langan and F. K. Garas, "The failure of concrete under the combined action of high shearing forces and biaxial restraint", Conference on Structures, Solid Mechanics and Engineering Design, Southampton, Paper 85, 1969.

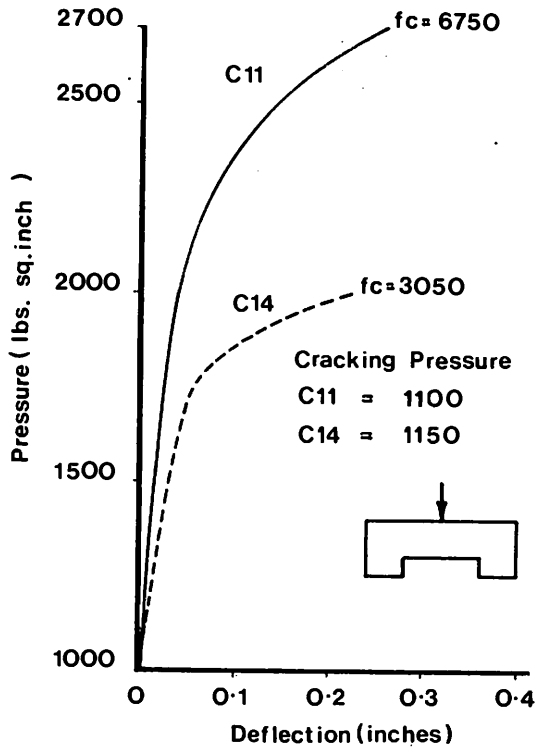


Fig. 1 - Effect of Concrete Strength on Central Deflection

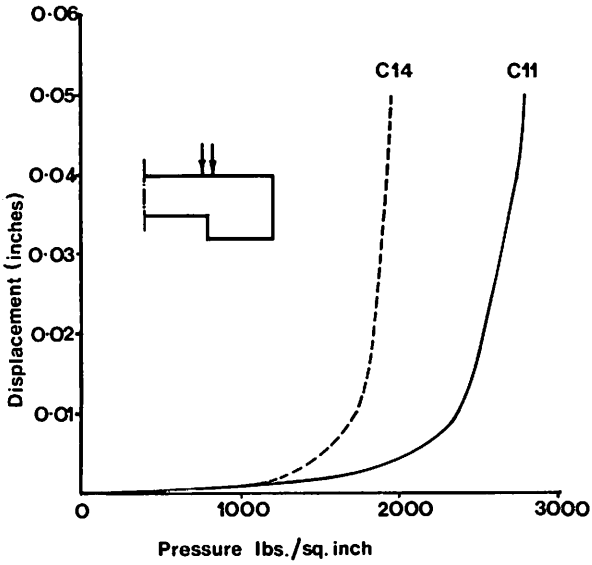


Fig. 2 - Effect of Concrete Strength on Shear Deformation

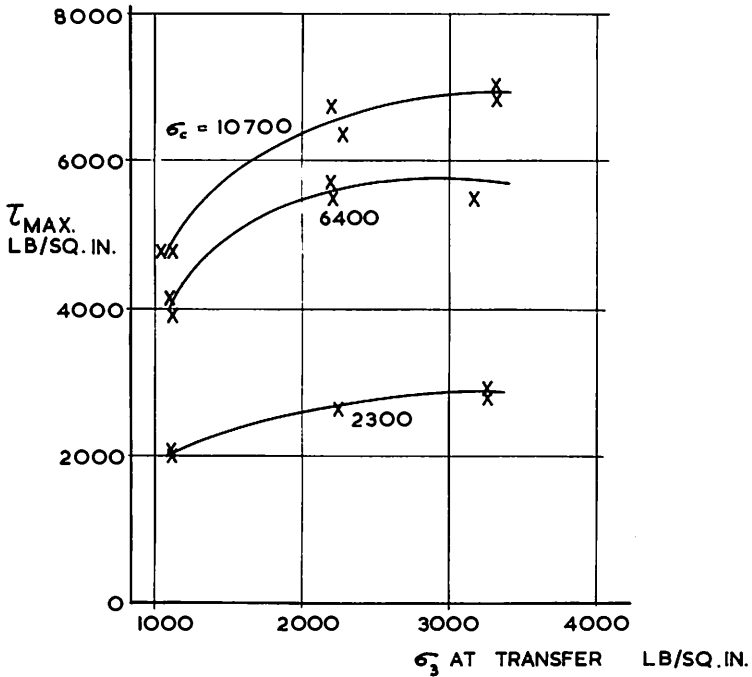


Fig. 3 - Effect of Concrete Strength on Shear Strength of 9x5 5/8" Concrete Specimens

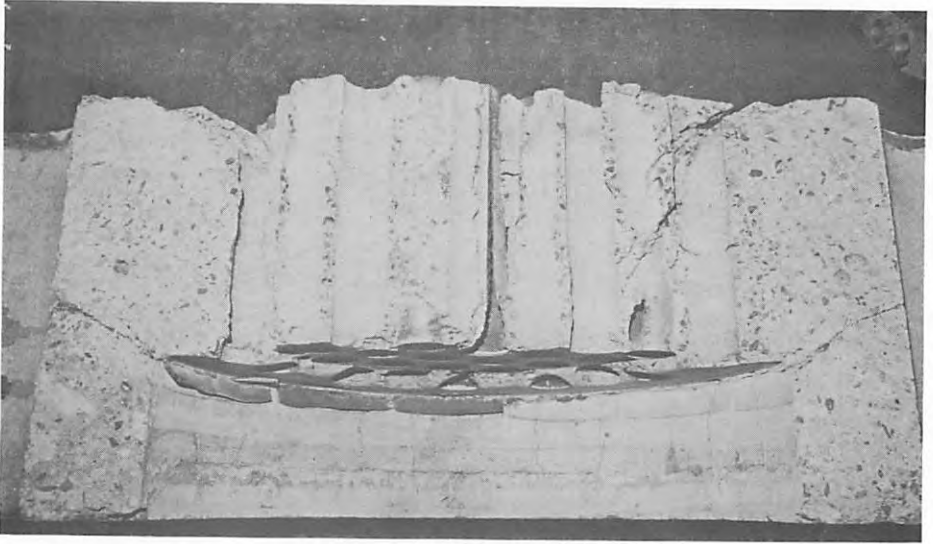


Fig. 4 - Cross Section of Model MO

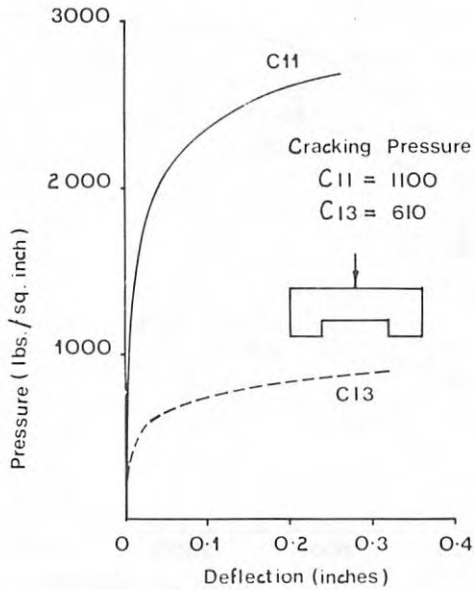


Fig. 5 - Effect of Hoop Prestress on Central Deflection

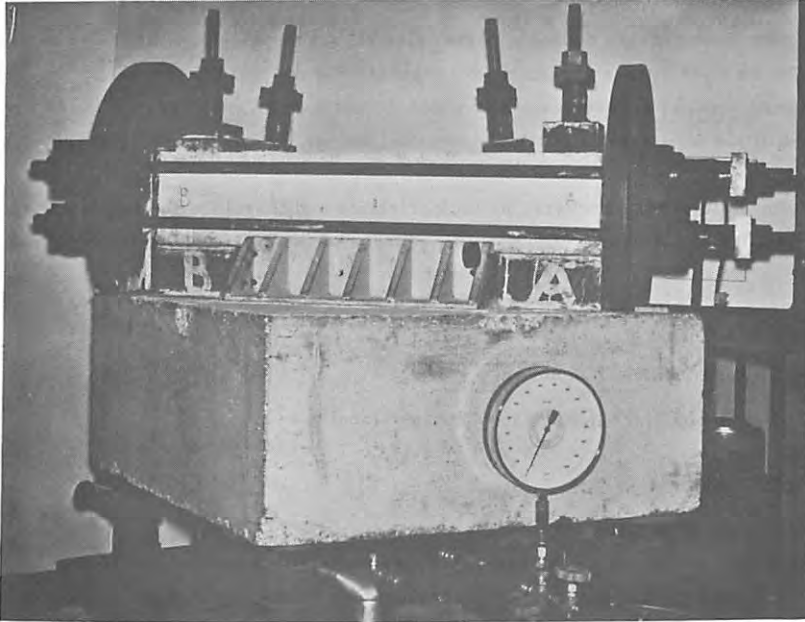


Fig. 6 - Shear Beam - Test Arrangement

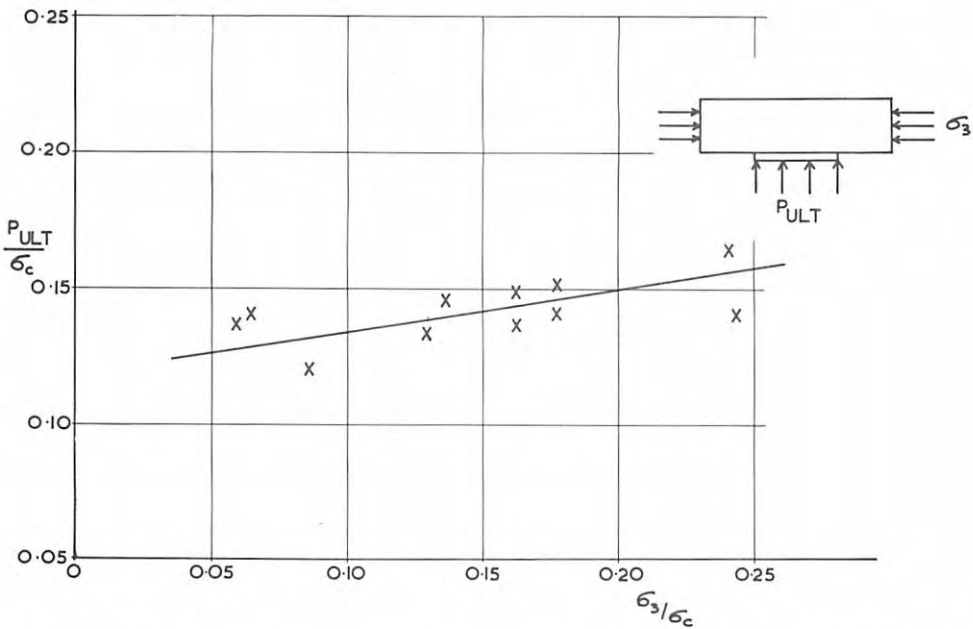


Fig. 7 - Restraint v Pressure for Beams with Span/Depth Ratio of 2.5

F. SCOTTO, Italy

C

We have carried out many tests on small scale cap-slabs-rings and entire PCP vessels, and we have always carefully investigated what we call the "reversibility limit" referred to the limit of pressurisation at which dropping down the pressure in the operating limits, even if the structure is cortically cracked we can find the previous quasi-elastic behaviour.

I belong to the field of the purchaser of nuclear plants and therefore the importance of knowing the reliability of the vessel (and per consequence of the entire plant) is obvious in case of accident.

Y. R. RASHID, U. S. A.

Q

How was failure defined in this experiment ?

D. LANGAN, U. K.

A

Criterion of failure ?

For the tests we carried out on the two 1/5 Bugey models failure was considered as reached when we could not increase any more the pressure due to the fact that the outflow of water (or oil) through the cracks was equal to the outflow of the hydraulic pumps used for the test. Of course this is not true for a gas pressure test.